Chemistry & Biology
Article

Discovery of Oxysterol-Derived Pharmacological Chaperones for NPC1: Implication for the Existence of Second Sterol-Binding Site

Kenji Ohgane,[1,*] Fumika Karaki,[1] Kosuke Dodo,[2] and Yuichi Hashimoto[1]
[1]Institute of Molecular and Cellular Biosciences, The University of Tokyo, Bunkyo-ku, Tokyo 113-0032, Japan
[2]RIKEN, Wako, Saitama 351-0198, Japan
*Correspondence: ohgane@me.com
http://dx.doi.org/10.1016/j.chembiol.2013.02.009

SUMMARY

Niemann-Pick type C1 (NPC1) is a polytopic endosomal membrane protein required for efflux of LDL-derived cholesterol from endosomes, and mutations of this protein are associated with Niemann-Pick disease type C, a fatal neurodegenerative disease. At least one prevalent mutation (I1061T) has been shown to cause a folding defect, which results in failure of endosomal localization, leading to a loss-of-function phenotype. Here, we show that several oxysterols and their derivatives act as pharmacological chaperones; binding of these compounds to I1061T NPC1 corrects the localization/maturation defect of the mutant protein. Further, these compounds alleviate intracellular cholesterol accumulation in patient-derived fibroblasts, suggesting that they may have therapeutic potential. These oxysterol derivatives bind to a domain of NPC1 that is different from the known N-terminal sterol-binding domain; i.e., there is an additional sterol-binding site on NPC1.

INTRODUCTION

Niemann-Pick disease type C (NPC) is a fatal, autosomal recessive neurodegenerative disease, characterized by massive cholesterol accumulation in lysosomes and late endosomes (Patterson et al., 2001). Approximately 95% of NPC patients have a mutation in the gene encoding Niemann-Pick type C1 protein (NPC1) (Ory, 2000), which is a late-endosomal protein with 13 transmembrane-spanning domains (Carstea et al., 1997; Loftus et al., 1997; Davies and Ioannou, 2000). The remaining 5% of patients have mutations in NPC2, a soluble, cholesterol-binding, late-endosomal protein (Naureckiene et al., 2000). Loss of function of either NPC1 or NPC2 results in indistinguishable phenotype, and these proteins are both considered to participate in intracellular cholesterol trafficking in a concerted manner (Sleat et al., 2004).

Although it is clear that NPC1 is essential for the egress of lipoprotein-derived cholesterol from endosomes, the mechanism of cholesterol export remains to be clarified in detail. Binding of cholesterol, oxysterols, and fluorescent sterols to NPC1 protein has been demonstrated by several groups (Ohgami et al., 2004; Infante et al., 2008a; Liu et al., 2009a), and the binding site of sterols has been determined to be a soluble N-terminal domain (NTD) (Infante et al., 2008b; see also Figure 1A). Subsequently, crystal structures of the NTD complexed with cholesterol and 25-hydroxycholesterol (25HC) were solved (Kwon et al., 2009), and the importance of this domain in NPC1-dependent transport of cholesterol was demonstrated in vivo (Xie et al., 2011). Taking into account the reported cholesterol transfer between NTD and NPC2 (Infante et al., 2008c), the mechanism of cholesterol transport is proposed to be as follows: (1) cholesterol-bound NPC2 binds to luminal loop 2 of NPC1 (Deffieu and Pfeffer, 2011), (2) cholesterol slides into the cavity of the NTD from NPC2 in a mouth-to-mouth manner (a hydrophobic hand-off model) (Wang et al., 2010), and (3) cholesterol is transferred to an unknown cytosolic acceptor molecule(s).

To date, more than 100 disease-causing mutations in NPC1 have been reported (OMIM 607623). At least for the most prevalent mutation, I1061T, the molecular mechanism of loss of function has been proposed to involve a folding defect and increased instability, rather than an intrinsic loss of function (Gelsthorpe et al., 2008). This mutant has lower folding efficiency and is retained in the endoplasmic reticulum (ER), a site of folding and quality control of membrane proteins, as a result of recognition by the cellular quality control system, consequently being targeted for proteasomal degradation. As a result of ER retention and rapid degradation, the level of functional NPC1 in the late endosomes decreases, and this results in loss-of-function phenotype. Although a large proportion of the mutant protein shows the trafficking defect and is degraded in the ER, a small proportion of the protein does fold correctly and is localized to late endosomes. The correctly localized mutant protein has also shown to be intrinsically functional with respect to cholesterol transport.

Considering the folding-defective nature of the NPC1 mutant protein, one possible approach to treat NPC is to identify pharmacological chaperones, i.e., small-molecular ligands that correct the trafficking defect resulting from the lower folding efficiency, presumably by binding to the folding intermediate in the ER (Loo and Clarke, 1997) and encouraging its escape from the ER quality control system (Ishii et al., 1993; Morello et al., 2000a, 2000b; Fan, 2003; Loo and Clarke, 2007).

Here, we report that 25HC acts as a pharmacological chaperone, enhancing the folding/maturation and correcting the trafficking defect of NPC1^{I1061T} mutant. Based on this finding, we

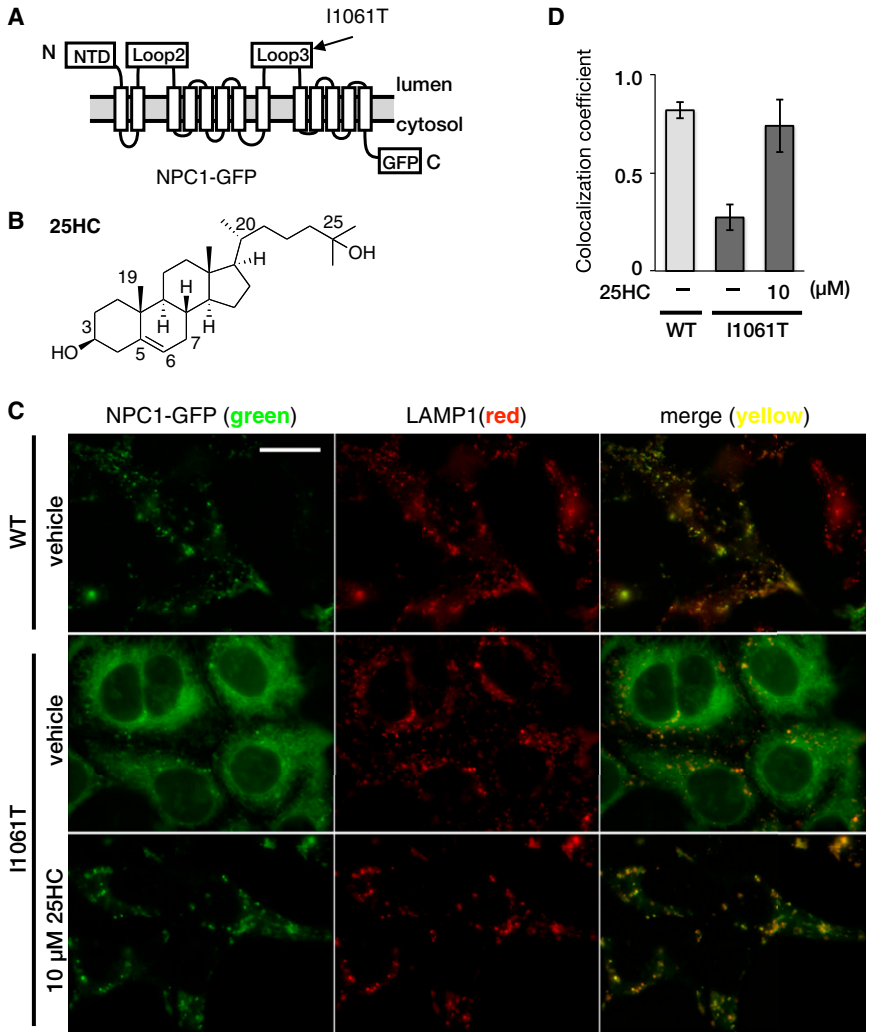

Figure 1. Correction of Subcellular Localization of NPC1^{I1061T} Mutant by 25HC

(A) Schematic representation of the predicted topology of the NPC1 protein. The three large luminal loops are denoted as NTD, loop 2, and loop 3. Loop 3 harbors the I1061T mutation.

(B) Structure of 25HC, showing relevant carbon numbers.

(C) Subcellular localization of WT and I1061T mutant NPC1-GFP, and effect of 25HC on NPC1^{I1061T}-GFP localization. HEK293 cells stably expressing the indicated construct were incubated with 25HC for 24 hr, and the localization of NPC1-GFP and LAMP1 was examined. Calibration bar represents 20 μm.

(D) Quantitative analysis of colocalization between NPC1-GFP proteins and LAMP1. The images obtained as in (C) were analyzed as described in Experimental Procedures. Data points represent the mean with SD depicted by error bars (n = 5).

conducted structure-activity relationships studies, which led to the identification of highly potent pharmacological chaperones. We also examined the functional consequence of pharmacological chaperone treatment of NPC patient-derived fibroblasts, which harbor I1061T mutation on both alleles, and found that cholesterol accumulation was alleviated. In the course of the structure-activity relationships studies, we noticed inconsistency between the reported crystal structure of NTD and the obtained structure-activity relationships, leading us to hypothesize that NPC1 has a second sterol-binding site, other than the NTD. Here, we provide unequivocal evidence of the existence of this second, non-NTD sterol-binding site in NPC1.

RESULTS

Oxysterols Correct Subcellular Localization of Folding-Defective NPC1^{I1061T} Mutant

We first tested whether 25HC could act as a pharmacological chaperone for NPC1 protein by examining the effect of 25HC on NPC1^{I1061T}-GFP localization. Although the localization of NPC1^{WT}-GFP was LAMP1-positive late endosomes, a large proportion of NPC1^{I1061T}-GFP exhibited a perinuclear reticular pattern, characteristic of ER-retained proteins, and only a small proportion was correctly localized to LAMP1-positive late endosomes, as previously reported (Figure 1C) (Neufeld et al., 1999; Zhang et al., 2001a; Gelsthorpe et al., 2008). Upon treatment with 25HC, the steady-state localization of the mutant protein became vesicular, and the mutant protein was well colocalized with LAMP1, indicating recovery of the proper localization (Figure 1C). The extent of colocalization was quantified and shown in Figure 1D. Furthermore, as shown in Figure 2B, dose-dependent recovery of proper localization of NPC1^{I1061T} was observed, and the EC_{50} was estimated as 2.4 μM.

Next we explored the structure-activity relationship of the oxysterol-mediated change in NPC1^{I1061T} localization by testing a panel of oxysterols with one or two additional hydroxyl group(s), other than the 3-hydroxyl group. Among the tested oxysterols, 19-hydroxycholesterol (19HC) (Figure 2B) and 20(S)-hydroxycholesterol (data not shown) had no effect on NPC1^{I1061T}-GFP localization at 10 μM, whereas B-ring-hydroxylated sterols, such as 7β-hydroxycholesterol, showed activity comparable to or slightly higher than that of 25HC (data not shown).

Identification of Potent Oxysterol Derivatives through Chemical Optimization

To identify more potent oxysterol derivatives, we conducted cycles of synthesis and evaluation using the NPC1^{I1061T} localization assay (data not shown), and identified potent oxysterol derivatives with more than one order of magnitude lower EC_{50} values. For example, the EC_{50} of mo56CFA, one of the most potent derivatives, was 0.12 μM, and this is nearly 20-fold lower concentration compared to 25HC. Structures and EC_{50} values of representative compounds are shown in Figure 2 (see also

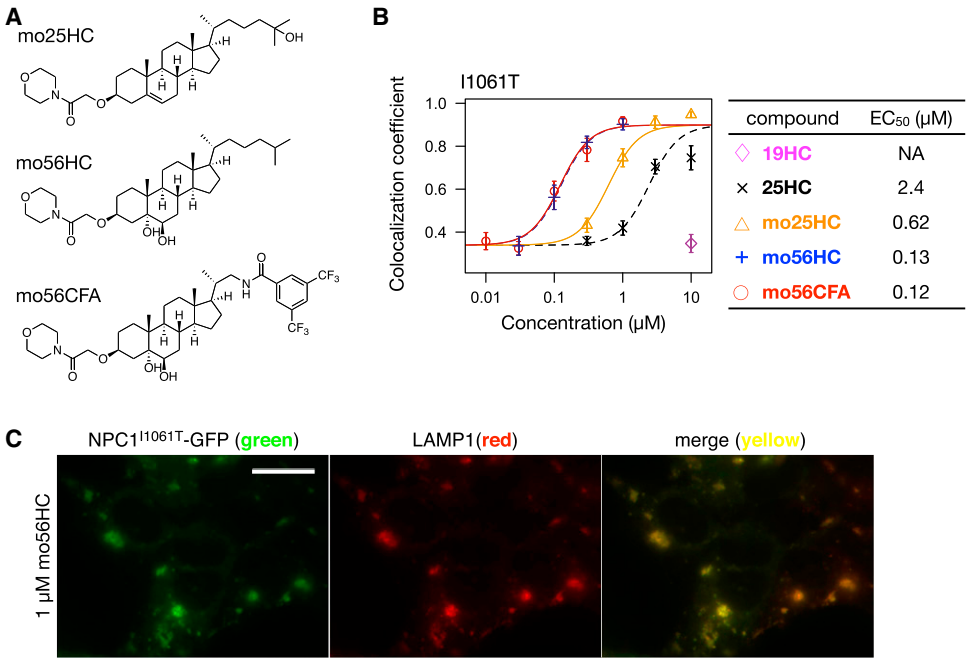

Figure 2. Identification of Sterol Derivatives with Greater Potency by Means of Chemical Optimization

(A) Structures of representative sterol derivatives used in this article.

(B) NPC1^{I1061T} colocalization assay, showing dose-response curves for selected oxysterols and sterol derivatives. The extent of colocalization of the NPC1 mutant and LAMP1 was quantified as described in Experimental Procedures, and the data points represent the averages (n = 10) with SE depicted by error bars.

(C) Representative images of the experiments in (B). Calibration bar represents 20 μm.

See also Figure S1A.

Figure S1A available online). Furthermore, the obtained derivatives did not correct mislocalization of another folding-defective protein, rhodopsin P23H mutant, indicating specificity of the effect (Figure S1B). This data supports the hypothesis that these compounds act as pharmacological chaperones.

Oxysterol Derivatives Stabilize NPC1^{I1061T} Mutant Protein and Increase its Steady-State Level

NPC1^{I1061T} mutant is unstable because of accelerated degradation at the ER, resulting in lower steady-state levels (Gelsthorpe et al., 2008; Yamamoto et al., 2000, 2004; Ninomiya, 2006). In the case of G protein-coupled receptors (GPCRs), it has been shown that unstable mutant receptors can be stabilized in cells by adding their ligand, and upregulation of the steady-state levels of the receptors can be used as a method for detecting ligand binding (MacEwan and Milligan, 1996; Ramsay et al., 2001). To examine whether oxysterol derivatives stabilize the mutant protein and eventually increase its steady-state level, we studied NPC1^{I1061T}-GFP expression levels by measuring the GFP fluorescence. As shown in Figure 3A, mo56CFA dose-dependently increased the level of NPC1^{I1061T} protein, whereas no significant increase was observed for the wild-type (WT) protein. As a control for those experiments, identical experiments were performed using 19HC, one of the inactive oxysterols, and no significant upregulation was observed (Figure 3A). Furthermore, the relative efficacies of the oxysterol derivatives in this assay were the same as those in the localization assay (Figures 2B and 3A). These results support the notion that the observed upregulation is a result of ligand-mediated stabilization resulting from binding of the oxysterol derivatives to the NPC1^{I1061T} mutant protein.

Oxysterol Derivatives Promote Maturation of NPC1^{I1061T} Mutant

Next, we examined the effect of oxysterol derivatives on NPC1^{I1061T} maturation by monitoring the EndoH sensitivity. EndoH can hydrolyze only unmodified *N*-linked glycans, and sensitivity to this enzyme indicates that the proteins are immature and have not exited from the ER. In accordance with a previous report (Gelsthorpe et al., 2008), NPC1^{I1061T}-GFP digested with EndoH migrated faster on SDS-PAGE than EndoH-resistant WT protein (Figure 3B). Upon treatment with 25HC or mo25HC, NPC1^{I1061T}-GFP became resistant to EndoH, indicating that oxysterols and oxysterol derivatives promote maturation of NPC1^{I1061T} proteins.

Bifunctional Photoaffinity Probe Reveals Direct Binding of Oxysterol Derivatives to NPC1

To test the hypothesis that the observed effects of oxysterol derivatives on NPC1^{I1061T} mutant proteins are mediated through direct binding to NPC1 (i.e., oxysterol derivatives act as pharmacological chaperones), we synthesized a bifunctional photoaffinity probe, mo56AZK (Figure 4A), and conducted photoaffinity labeling experiments (Hosoya et al., 2004). This compound contains an aryl azide as a photoreactive group and an alkyne for conjugation with a reporter molecule, such as biotin, by Cu-catalyzed azide-alkyne cycloaddition (CuAAC) (MacKinnon et al., 2007; Ban et al., 2010; Côté et al., 2011). The small size

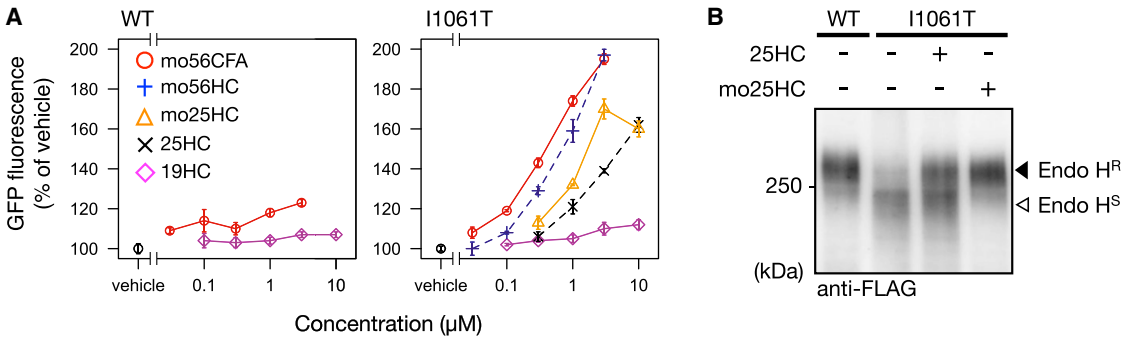

Figure 3. Effect of Oxysterol Derivatives on Steady-State Expression Level and Maturation Status of NPC1^{I1061T} Mutant

(A) The steady-state expression level of FLAG-NPC1-GFP (WT or I1061T) was quantified by measuring GFP fluorescence in the lysate with or without oxysterol derivatives. The GFP fluorescence was normalized with respect to total protein concentration. Data points represent the averages (n = 3) with SD depicted by error bars.

(B) Acquisition of EndoH resistance upon treatment with 25HC and its derivative. Cells stably expressing either WT or I1061T version of FLAG-NPC1-GFP were treated as indicated for 24 hr and lysed. The lysates were digested with EndoH and immunoprecipitated with anti-FLAG beads. The immunoprecipitated proteins were subjected to western blot analysis (immunoblotted with anti-FLAG antibody).

of both azide and alkyne groups allowed us to obtain this probe (EC_{50} 0.078 μM) without loss of activity compared with the parental compound mo56CFA (EC_{50} 0.12 μM) (Figures 2B and 4B). Next, we used this probe to examine whether the oxysterol derivatives directly bind to NPC1 by means of photocrosslinking experiment. As shown in Figures 4C and 4D, mo56AZK directly labeled NPC1 upon UV irradiation, and the fact that the labeling was subject to competition by mo56CFA indicates the specificity of this crosslinking reaction.

Similar experiments with I1061T mutant gave essentially the same results (data not shown; cf. Figure 7C), demonstrating that the binding of mo56AZK was independent of the presence or absence of the I1061T mutation. Thus, direct interaction between the oxysterol derivatives and NPC1 proteins was demonstrated. This result strongly supports our hypothesis that these compounds act as pharmacological chaperones for the I1061T mutant.

Oxysterol Derivatives Promote Maturation of Endogenous NPC1^{I1061T} in Patient-Derived Fibroblasts

It has been reported that I1061T and some other mutants show altered band patterns on western blots, with smaller apparent molecular mass (Watari et al., 1999a, 1999b) (Figure 5A). Furthermore, these smaller forms of NPC1 proteins were considered to be nonfunctional, based on the fact that the sterol-trafficking defect of CT60 cells, a CHO cell line lacking functional NPC1,

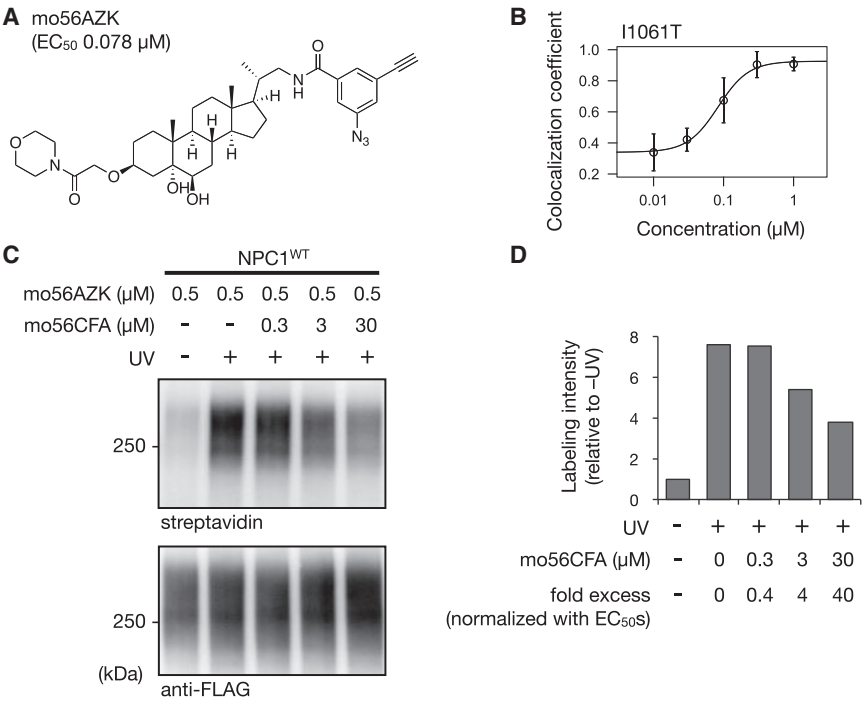

Figure 4. Direct Binding between Oxysterol Derivatives and NPC1

(A) Structure and EC_{50} value of bifunctional photoaffinity probe mo56AZK.

(B) mo56AZK dose-dependently rescue the localization defect of I1061T mutant. The data points represent the averages (n = 10) with SD depicted by error bars. See also Figure S1A.

(C) The probe mo56AZK specifically labels FLAG-NPC1-GFP. Photocrosslinking experiments were performed as described in Experimental Procedures.

(D) The quantified result of (C).

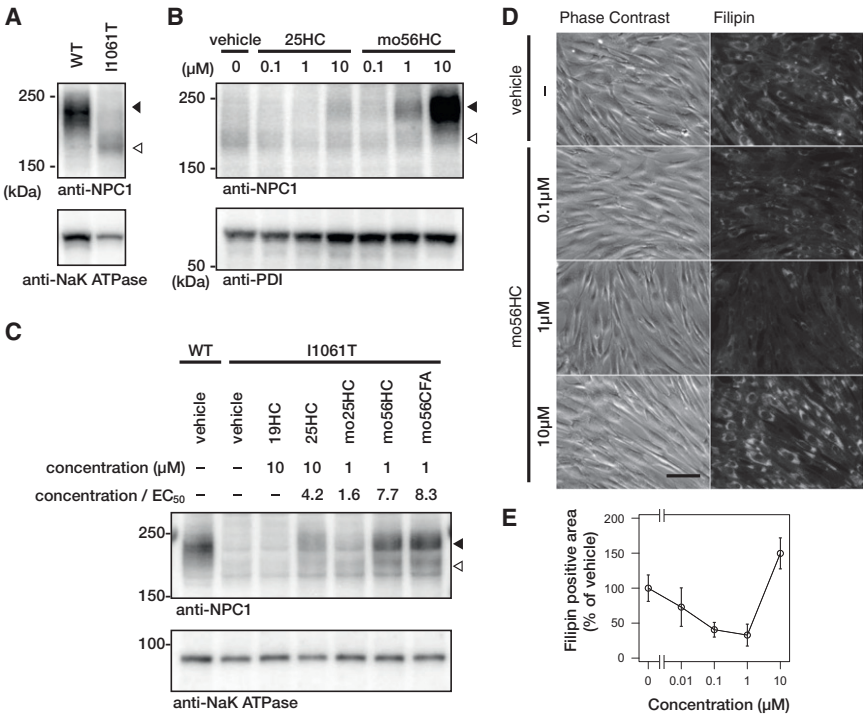

Figure 5. Functional Rescue of Patient-Derived Fibroblasts

(A) Comparison of the expression levels and band patterns of endogenous WT (HEK293) and I1061T NPC1 proteins (NPC fibroblast). The filled arrowhead indicates the mature form, and the open arrowhead indicates the immature form.

(B) Effects of 25HC and mo56HC on expression level and band pattern of endogenous NPC1^{I1061T}. NPC fibroblasts were treated with the indicated compound for 48 hr and processed for western blot analysis using anti-NPC1 antibody.

(C) Effect of other sterol derivatives on expression level and band pattern of I1061T mutant. To facilitate comparison between the compounds, the concentrations normalized with their EC_{50}s are also shown.

(D) Alleviation of intracellular cholesterol accumulation by oxysterol derivative. NPC fibroblasts were cultured in the presence of the indicated compound for 48 hr, and processed for filipin staining. Calibration bar represents 100 μm. The intracellular cholesterol accumulation was quantified as described in Experimental Procedures. Error bar represents SD (n = 12).

See also Figure S2.

could not be corrected by transfection of the cells with these mutants (Watari et al., 2000). Here, we explored whether treatment with oxysterol derivatives could normalize the altered band pattern of endogenous NPC1^{I1061T} mutant protein by using NPC patient-derived fibroblasts with the I1061T mutation on both alleles. When NPC fibroblasts were treated with mo56HC, a dose-dependent increase in expression level and a band shift toward higher molecular weight were observed, so that the band pattern became nearly the same as that of WT protein (Figures 5B and 5C). Treatment with 25HC also increased the abundance of the higher-molecular-weight species, although more than 10-fold higher concentration was required in this case (Figures 5B and 5C). For other oxysterol derivatives, the relative efficacies in the NPC1 localization assay were recapitulated; the upregulation was detectable only when the concentrations higher than their EC_{50}s were used. (Figure 5C). Considering the results obtained from cells overexpressing NPC1^{I1061T}-GFP (Figures 1, 2, 3, and 4), these results suggest that the oxysterol derivatives stabilized and promoted the maturation of endogenous NPC1^{I1061T} protein in the patient-derived fibroblasts.

Oxysterol Derivatives Alleviate Intracellular Cholesterol Accumulation in Patient-Derived Fibroblasts

To examine whether the oxysterol-derived pharmacological chaperones could functionally rescue NPC1^{I1061T} protein, we evaluated their effect on intracellular cholesterol accumulation in NPC fibroblasts. When stained with filipin, a fluorescent polyene antibiotic with affinity for free cholesterol, NPC fibroblasts showed an intense intracellular staining pattern, indicating cholesterol accumulation in the lysosomes and late endosomes (Pentchev et al., 1985). Upon treatment with mo56HC (~1 μM), dose-dependent alleviation of this intracellular cholesterol accumulation was observed. As mo56HC did not downregulate LDL receptor nor inhibit LDL uptake (Figures S2C and S2D), this result indicates functional rescue of the NPC1^{I1061T} mutant protein by mo56HC (Figures 5D and 5E). Unexpectedly, however, a high concentration (10 μM) of mo56HC induced an increase of intracellular cholesterol accumulation compared with the vehicle-treated cells. One possible explanation of this result is that the observed accumulation is due to an inhibitory effect of mo56HC on NPC1 function at high concentration.

The Presence of NTD Is Not Obligatory for Sterol-Mediated Rescue of NPC1^{I1061T} Localization Defect

Our structure-activity relationship studies on oxysterol derivatives revealed that (1) introduction of a substituent on the 3β-hydroxyl group lowered EC_{50} by one order of magnitude in several series of derivatives (e.g., compare 25HC and mo25HC, Figure 2B), and (2) introduction of hydroxyl functionalities into the B-ring of the sterol, especially at the 5-, 6-, or 7-position, did not result in any loss of activity. On the other hand, the reported crystal structure of NTD complexed with 25HC showed that (1) 25HC binds to NTD with the 3β-hydroxyl group located deep in the binding pocket, and (2) the B-ring of 25HC is surrounded by hydrophobic residues, such as Leu, Phe, and Ile (Kwon et al., 2009). Thus, there appeared to be a discrepancy between our structure-activity relationships and the reported crystal structure. This discrepancy led us to explore the possibility that the binding site of our oxysterol derivatives is not situated in the NTD.

To address this possibility, we tested whether the oxysterol derivatives could correct the localization defect of NTD-deleted NPC1^{I1061T}-GFP (ΔNTD-I1061T) (Figure 6). Although a small proportion of full-length I1061T mutant shows late endosomal distribution, ΔNTD-I1061T was completely localized to the ER. This observation indicates that the deletion of the NTD itself

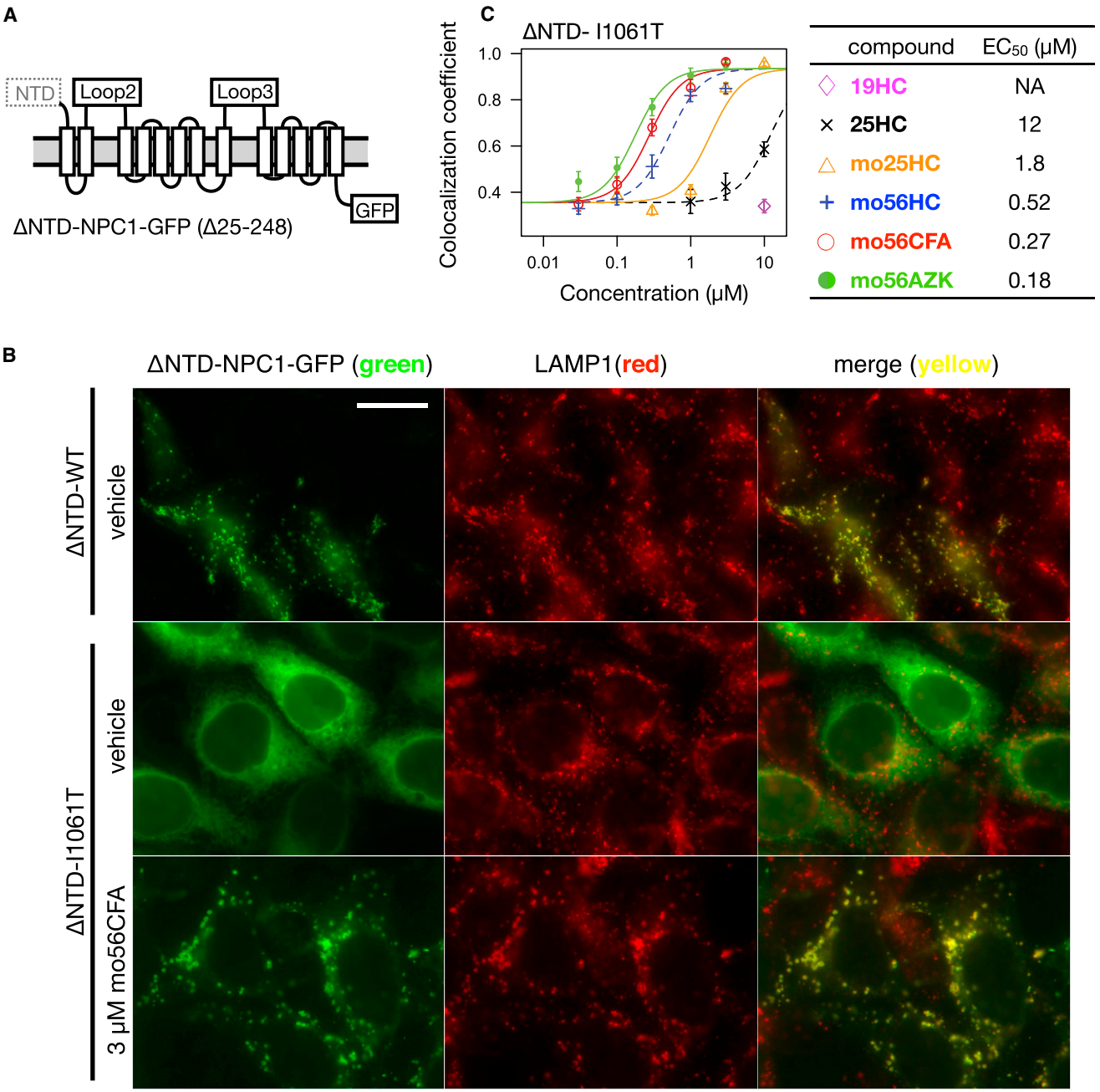

Figure 6. Dispensability of NTD for Oxysterol Derivative-Mediated Rescue of Mutant NPC1 Protein

(A) Schematic representation of the NTD-deleted NPC1-GFP (ΔNTD).

(B) Subcellular localization of the ΔNTD-WT and ΔNTD-I1061T. Cells stably expressing the ΔNTD-NPC1-GFP construct were treated as indicated for 24 hr and colocalization of the NPC1 with LAMP1 was examined. Calibration bar represents 20 μm.

(C) Dose-dependent rescue of ΔNTD-I1061T localization by representative oxysterol derivatives. The graph shows the dose-response curves of representative compounds and the table shows calculated EC_{50} values. For 25HC, the extrapolated value is shown. Error bar, SE (n = 12).

slightly reduced the folding efficiency. In spite of this diminished folding efficiency, the ER localization of ΔNTD-I1061T was efficiently corrected to late endosomal localization by treatment with the oxysterol derivatives (Figure 6B), demonstrating that the NTD is not required for the pharmacological chaperone effect. We further characterized this effect by determining the EC_{50} values of the oxysterol derivatives. As shown in Figure 6C, the rank order of the derivatives was the same as in Figure 2B, showing the same specificity as with the full-length protein. Compared with full-length I1061T, however, we observed rightward shifts of the dose-response curves for ΔNTD-I1061T. Taking into account the observation that deletion of the NTD itself slightly lowered the folding efficiency, we rationalized these rightward shifts as reflecting decreased folding efficiency. These

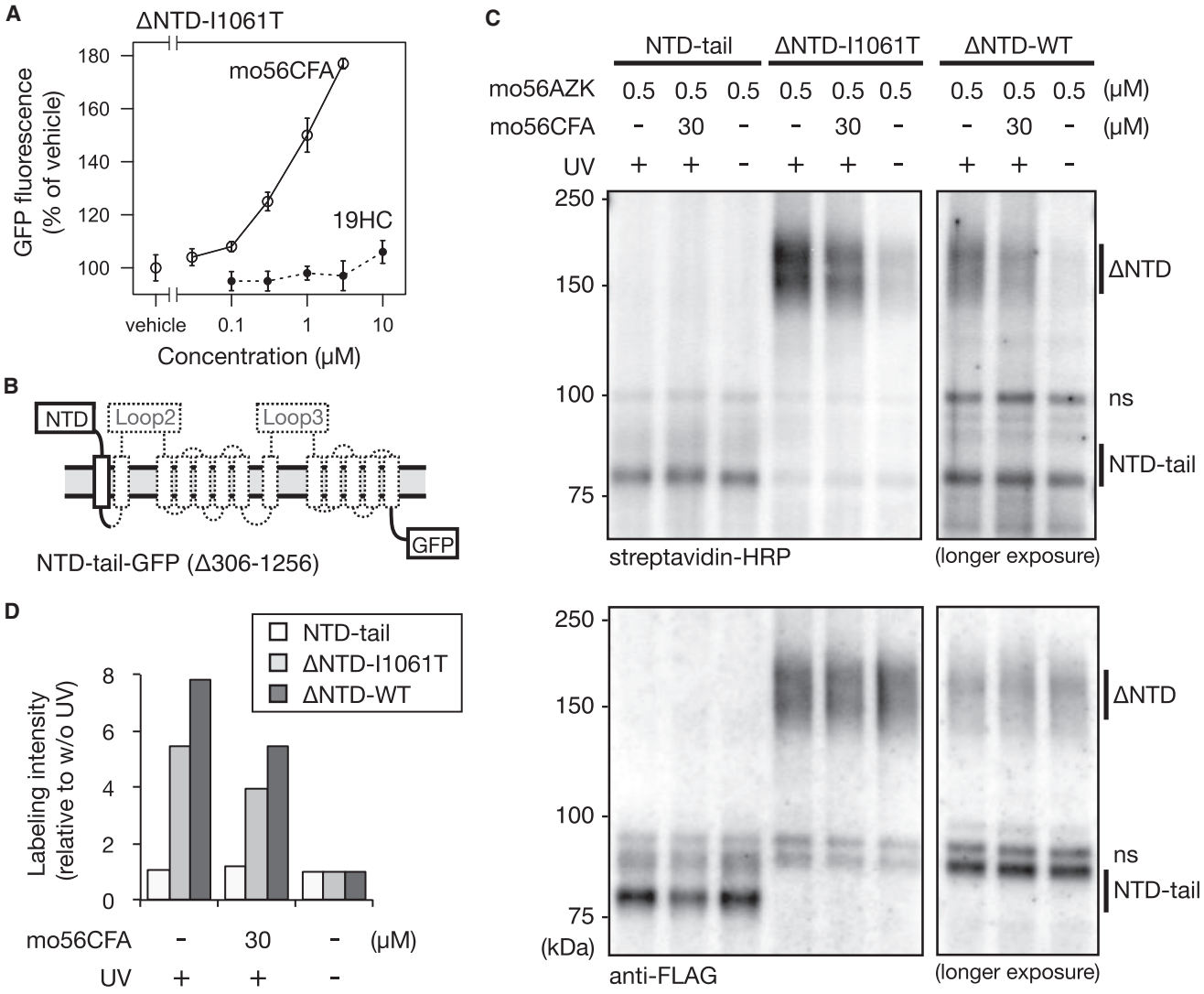

Figure 7. Existence of Non-NTD Sterol-Binding Site

(A) Sterol-mediated stabilization of ΔNTD-I1061T. The steady-state expression level of ΔNTD-I1061T was quantified as in Figure 3A. Error bar, SD (n = 3).

(B) Schematic representation of the NTD-tail-GFP construct. See also Figure S3.

(C) Photoaffinity labeling experiments of NTD-deleted NPC1 and NTD-tail NPC1. Membranes from cells stably expressing either FLAG-tagged ΔNTD-I1061T or NTD-tail-GFP were labeled with mo56AZK as in Figure 4. Right panel shows the labeling of ΔNTD-WT. Because of the low expression level of the stable cell line, the longer exposure time was used for ΔNTD-WT. ns, nonspecific labeling/staining. See also Figure S3C.

(D) The quantified results of (C).

data clearly point to the existence of a sterol-binding site that is distinct from the NTD.

Oxysterol-Derived Pharmacological Chaperones Stabilize NTD-Deleted NPC1^{I1061T} Mutant

To test whether the stabilizing effect of the oxysterol derivatives on I1061T mutant was also independent of the existence of NTD, we examined the steady-state levels of ΔNTD-I1061T. As had been found for full-length I1061T, mo56CFA stabilized ΔNTD-I1061T protein in a dose-dependent manner, but 19HC did not (Figure 7A). Furthermore, the relative efficacies of other oxysterol derivatives were also consistent with those in the case of full-length I1061T mutant (data not shown). These data strongly support the hypothesis that the oxysterol-derived pharmacological chaperones bind to a distinct, non-NTD sterol-binding site on NPC1.

Oxysterol-Derived Pharmacological Chaperones Directly Bind to a Non-NTD Sterol-Binding Site

To demonstrate the direct binding of oxysterol derivatives to the putative non-NTD sterol-binding site, we again conducted photocrosslinking experiments. For this purpose, we used two cell lines stably expressing FLAG-tagged NPC1-GFP construct; one is ΔNTD (Δ25–248) and the other is NTD-tail (Δ306–1256) (Figure 7B). The latter construct contains the NTD, the first transmembrane domain, and the C-terminal tail, which is required for

endosomal localization (Watari et al., 1999a; Scott et al., 2004). The NTD-tail localized correctly to LAMP1-positive endosomes (Figure S3A), indicating that the protein structure is not compromised by this large deletion. As shown in Figures 7C and 7D, mo56AZK specifically labeled both ΔNTD-I1061T and ΔNTD-WT. On the other hand, neither UV-dependent labeling nor competition by mo56CFA could be observed for NTD-tail. This result clearly demonstrated that oxysterol derivatives directly and selectively bind to a non-NTD sterol-binding site. Thus, it is most likely that there exist additional sterol-binding site and that the observed effects of the oxysterol derivatives on NPC1^{I1061T} mutant protein are mediated through direct binding of the compounds to this non-NTD sterol-binding site.

DISCUSSION

Our data clearly support the following two propositions: (1) oxysterols and their derivatives act as pharmacological chaperones for NPC1^{I1061T} mutant, and (2) their binding site is not the known sterol-binding domain, NTD, but another, distinct binding site on NPC1.

To date, much effort has been made to elucidate the etiology of NPC and to gain insight into NPC1 function. Recent progress has provided some promising therapeutic options, such as cyclodextrin treatment and substrate reduction therapy (Rosenbaum and Maxfield, 2011). Cyclodextrins have been shown to reduce the NPC phenotype and to prolong the lifespan of *npc1*$^{-/-}$ mice, possibly via cyclodextrin-mediated clearance of endosomal cholesterols (Griffin et al., 2004; Davidson et al., 2009; Liu et al., 2009b; Aqul et al., 2011). Another therapeutic option, substrate reduction therapy, is based on the fact that glycosphingolipids also accumulate in late endosomes. To alleviate the accumulation of glycosphingolipids, which may affect neuronal viability, a glucosylceramide synthase inhibitor, miglustat, has been tested, and it was shown to improve several clinical markers (Patterson et al., 2007).

Our approach here was to find compounds that alleviate the folding defect of NPC1 mutant proteins, such as I1061T. Here, we successfully found that some oxysterols and their more potent derivatives can act as pharmacological chaperones, and our results demonstrate the potential value of this strategy as an option for NPC treatment. Recently, histone deacetylase (HDAC) inhibitors have been shown to upregulate NPC1 expression level via transcriptional regulation of HDAC target genes, and functional rescue in NPC fibroblast has also been achieved (Pipalia et al., 2011). As the pharmacological chaperones act posttranslationally, the combination of HDAC inhibitors and the pharmacological chaperones may be of greater benefit.

Until now, two independent groups have purified NPC1 protein and conducted binding assay with ^{3}H-labeled sterols or fluorescent sterol analogs (Infante et al., 2008a; Liu et al., 2009a). The former group localized the binding site of sterols to the NTD and clearly demonstrated high-affinity binding between purified NTD and ^{3}H-labeled sterols (K_d 10 nM for 25HC). The latter group demonstrated binding between full-length NPC1 and fluorescent sterols by utilizing the change in fluorescence intensity of the sterols themselves upon binding to the purified protein as well as the change in intrinsic Trp fluorescence of NPC1 upon binding of the sterols. As regards the Trp fluorescence quenching, however, the former group mentioned that in their preliminary study they could not detect Trp fluorescence quenching of the NTD upon binding of 25HC. This discrepancy might be attributable to the difference in the experimental conditions the two groups employed (Infante et al., 2008b). However, considering the existence of the second sterol-binding site on NPC1, another explanation for the discrepancy is now possible, i.e., that the Trp fluorescence quenching was a result of the fluorescent sterol binding to the second, non-NTD sterol-binding site. Although the location of the second sterol-binding site has yet to be determined, its identification will provide a basis for resolving the discrepancy, if one or more Trp residues are present near this binding site.

Infante et al. (2008b) reported that both full-length NPC1 and NTD bound [^{3}H]25HC with similar saturation kinetics, proposing the NTD as the sole oxysterol-binding site, at least under their experimental conditions. On the other hand, we have found clear evidence of binding of 25HC and other oxysterol derivatives to a second, non-NTD sterol-binding site. Our working hypothesis is that the NTD is a high-affinity sterol-binding site, whereas the non-NTD sterol-binding site is a low-affinity or transient sterol-binding site, because the EC_{50} of 25HC was of micromolar order in our cell-based assay. Accordingly, binding of [^{3}H]25HC to the non-NTD sterol-binding site might not have been detected in their in vitro binding assay that requires bound/free separation.

A region of five consecutive transmembrane domains (TM3-7) of NPC1, known as the sterol-sensing domain (SSD), was initially found in two proteins related to cholesterol homeostasis, HMG-CoA reductase and SREBP-cleavage activating protein (SCAP) (Hua et al., 1996). Thereafter, this family was expanded to include other proteins related to cholesterol sensing, synthesis, metabolism, and transport, including NPC1, NPC1-like 1, Patched, and 7-dehydrocholesterol reductase (Kuwabara and Labouesse, 2002). However, the function of SSD in general remains enigmatic. Although sequence conservation of the SSD in sterol-related proteins suggests that SSD might be a sterol sensor, there is no report of direct binding of SSD and sterols. Ohgami et al. (2004) indicated the importance of intact SSD for cholesterol binding to NPC1. In their work, photocrosslinking of NPC1 protein by ^{3}H-labeled 7,7-azi-cholestanol was diminished by introduction of an SSD mutation, P691S. The result clearly showed the requirement of intact SSD for sterol binding, but they did not establish whether the sterol directly bound to SSD or whether the SSD mutation affected the conformation of a sterol-binding site located somewhere other than in the SSD. In the case of NPC1, as mentioned above, a sterol-binding site was later localized to the NTD (Infante et al., 2008b). For SCAP, based on studies using purified SCAP, it is proposed that the cholesterol-binding site is not the SSD, but is a luminal loop adjacent to the SSD (Motamed et al., 2011), although this loop is not conserved in NPC1. Our data presented here demonstrate the existence of a distinct non-NTD sterol-binding site, and this may again raise the question of "does the SSD bind sterols"? Our on-going studies to establish the localization and identity of the second sterol-binding site should provide an answer to this question.

A question also arises as to whether this second sterol-binding site on NPC1 plays a role in NPC1 functions. In general, the effect of pharmacological chaperones on the function of a mutated

target protein is biphasic; at lower concentration they restore function to the mutant protein, but at higher concentration they inhibit the function by acting as inhibitors or antagonists. This appears to be the case for our sterol derivatives. As shown in Figure 5D, treatment with the sterol derivatives at lower concentration alleviated cholesterol accumulation in the endosomes of patient-derived fibroblasts, but a higher concentration, such as 10 μM, conversely induced accumulation of free cholesterol in the endosomes. Similar accumulation was also observed in other cells endogenously expressing $NPC1^{WT,}$ such as HEK293 cells (Figure S2). Further, we observed that the cells overexpressing $NPC1^{WT}$-GFP showed resistance to this sterol derivatives-induced accumulation of cholesterol (data not shown). Therefore, we think the mechanism of the cholesterol accumulation involves inhibition of NPC1 function, though other possibilities cannot be ruled out. These results suggest a functional significance of the second sterol-binding site.

It is still unclear how NPC1 regulates intracellular cholesterol trafficking. One possible mechanism is that NPC1 acts as a permease/transporter, and transport sterols or other substrates to the cytosolic face (Davies et al., 2000; Ioannou, 2001). This hypothesis is based on the fact that NPC1 shares sequence homology with prokaryotic resistance-nodulation division (RND) transporters, which are proton antiporters that mediate efflux of substances from cells (Tseng et al., 1999). Another possible mechanism is that NPC1 regulates intracellular lipid transport via regulation of vesicular trafficking (Ohsaki et al., 2006; Zhang et al., 2001b; Ko et al., 2001). The second sterol-binding site may be a substrate-binding site that channels sterols from the luminal to cytosolic face, or a regulatory site that controls vesicular trafficking in a sterol-dependent manner. These possibilities should be examined in the future.

In conclusion, we have discovered the oxysterol-derived pharmacological chaperones for folding-defective NPC1 mutant, and we have also uncovered the presence of a second sterol-binding site, distinct from the NTD site. Although further work is needed to establish the physiological significance of this site, our two-sites model is expected to provide a useful framework for understanding the function and regulation of NPC1 and other related proteins. The location of the second sterol-binding site remains to be identified. Work on these issues is under way.

SIGNIFICANCE

We report several oxysterols and their chemically optimized derivatives as pharmacological chaperones for NPC1 I1061T mutant. The mutant NPC1 protein is folding-defective, fails to achieve the usual endosomal localization, and is rapidly degraded at the ER, thus leading to loss-of-function phenotype. We found that oxysterol derivatives correct these phenotypes by directly binding to NPC1 protein. Furthermore, the N-terminal domain of NPC1, a well-established sterol-binding site, is not required for our oxysterol-derived pharmacological chaperones to bind to NPC1 and exert their effect. This result clearly indicates the existence of an additional, second sterol-binding site on NPC1. The original identification of the N-terminal domain as a sterol-binding site greatly improved our understanding of NPC1 function as a key molecule in egress of cholesterol from late endosomes. However, it remains elusive how NPC1 transports sterols beyond endosomal membranes. Our discovery of pharmacological chaperones and the putative second sterol-binding site should help to provide a rational basis for developing therapeutics, as well as for elucidating the still-enigmatic functions of NPC1 and other related proteins.

EXPERIMENTAL PROCEDURES

Cell Culture

HEK293 cells were cultured in Dulbecco's modified Eagle's medium (DMEM) supplemented with 5% fetal bovine serum (FBS) and penicillin and streptomycin at 37°C in a humidified incubator (5% CO_2). Cell lines stably expressing NPC1 construct were maintained in the presence of G418 (0.4 mg/ml). NPC patient-derived fibroblast cell line GM18453 was obtained from Coriell Institute. The fibroblasts were maintained in Eagle's minimal essential medium supplemented with 10% FBS and penicillin and streptomycin, and they were used for experiments within 9–11 passages.

DNA Constructs

The expression vector encoding NPC1 (GenBank BC063302.1) C-terminally tagged with turboGFP under control of the CMV promoter was purchased from OriGene. As previously reported, FLAG tag was inserted at the *ClaI* site by PCR mutagenesis; insertion at this site does not affect the localization or function of NPC1 (Davies and Ioannou, 2000; Ohsaki et al., 2006). Thus, our constructs contain an additional sequence DYKDDDDKI (FLAG tag and an Ile) between amino acid residues 305 and 306. Site-directed mutagenesis was conducted by inverse PCR using KOD-plus (Toyobo). The coding regions of the plasmids were sequenced and the integrity of each construct was confirmed.

Immunocytochemical Staining of LAMP1

Cells were fixed (3.7% formaldehyde in PBS, room temperature [rt], 30 min), permeabilized (0.1% Triton X-100 in PBS, rt, 10 min), and blocked in 1% BSA-PBST for 1 hr. The samples were incubated with mouse anti-LAMP1 (Abcam) for 2 hr, then washed with PBS. The samples were incubated with anti-mouse IgG AlexaFluor 546 (Invitrogen) for 1 hr and washed with PBS, and images were acquired using an IX70 inverted fluorescence microscope (Olympus) with a 100× objective.

NPC1 Colocalization Assay and Quantitative Image Analysis

At day 1, HEK293 cells stably expressing $NPC1^{I1061T}$-GFP or ΔNTD-$NPC1^{I1061T}$-GFP were plated onto a poly-D-lysine-coated glass-bottomed dish. At day 2, cells were treated with the test compounds prediluted with DMEM (final DMSO concentration was 0.1%). After 24 hr, cells were fixed and processed for immunostaining of LAMP1. For quantitative analysis of NPC1 colocalization with LAMP1, images of 10 different area were acquired, and thresholded Manders' coefficient ("colocalization coefficient" in the figure) was quantified. Automated quantification of the coefficient were performed employing NIH ImageJ software. After background correction and automatic thresholding, the coefficients were calculated for the pairs of thresholded images using JACoP plugin (Bolte and Cordelières, 2006).

Synthesis of Oxysterol Derivatives

Details of the synthetic procedures and characterization data are given in Supplemental Experimental Procedures.

Quantification of GFP Fluorescence in Lysates

For evaluation of steady-state NPC1-GFP expression levels, GFP fluorescence of the lysates was measured. In a 12-well plate, cells were cultured in medium without phenol red to 70% confluence and treated with vehicle or test compounds. After 24 hr, the cells were lysed in TNET buffer (1% Triton X-100, 25 mM Tris, 150 mM NaCl, 5 mM EDTA, pH 7.5) for 1 hr on ice. The debris was removed by centrifugation (13,500 rpm at 4°C for 5 min), and the fluorescence of the supernatant was measured with a Wallac 1420 multilabel counter (Perkin-Elmer Life Sciences). The total protein concentrations were

determined by BCA assay (Dojindo), and the fluorescence intensities were normalized.

Endoglycosidase H (EndoH) Digestion and Immunoblot Analysis

Cell lysates (20 μg total protein) were incubated for 1 hr at 37°C with EndoH (Roche) in citrate buffer (50 mM sodium citrate, pH 5.5) in the presence of protease inhibitor cocktail. The FLAG-tagged NPC1 proteins were immunoprecipitated with anti-FLAG M2 agarose (4°C, overnight), and eluted by incubation in Laemmli sample buffer at 60°C for 15 min. The samples were separated by SDS-PAGE (7.5%) and subjected to immunoblot analysis using anti-FLAG M2 antibody (from Sigma).

Photoaffinity Labeling and CuAAC

Membrane isolated from cells stably expressing FLAG-NPC1-GFP was incubated on ice with mo56AZK (0.5 μM) with or without competitor (30 μM mo56CFA) for 30 min, and irradiated with UV (365 nm) for 20 min at 0°C. The membrane was lysed and CuAAC reaction with biotin-azide was performed. From the reaction mixture, FLAG-NPC1-GFP was immunoprecipitated and separated on SDS-PAGE. After transfer to the PVDF membrane, the membrane was probed with streptavidin-HRP (Pierce) or anti-FLAG antibody (Sigma). For full protocol, see Supplemental Experimental Procedures.

Immunoblot Analysis

All samples involving NPC1 protein were prepared without boiling. Instead, lysates or immunoprecipitated proteins were heated at 60°C for 15 min with Laemmli sample buffer, and resolved by SDS-PAGE. For immunoblotting of endogenous NPC1 protein, rabbit anti-NPC1 polyclonal antibody (Novus Biologicals) combined with HRP-conjugated anti-rabbit antibody (R&D Systems) was used. For loading controls, rabbit anti-PDI antibody (Stressgen) or mouse anti-Na-K ATPase antibody (Abcam) was used.

Filipin Stain

At day 1, NPC fibroblasts were seeded onto glass-bottomed dishes. For filipin staining of HEK293 cells, poly-D-Lys-coated dishes were used. At day 2, test compounds prediluted in the medium (final DMSO concentration: 0.1%) were added. After the indicated time, cells were fixed (3.7% formaldehyde-PBS, rt, 30 min), washed (PBS), and stained with filipin III (50 μg/ml in 20% EtOH-PBS, rt, 45 min). The samples were washed with PBS, and images were acquired using 360/30 nm excitation and >420 nm emission filters (×20 objective for NPC fibroblasts or ×60 objective for HEK293 cells).

Quantification of Filipin-Positive Area

To quantify the extent of free cholesterol accumulation, we measured filipin-positive area. Acquired images were converted to binary by applying a threshold that discriminates filipin-positive, vesicular staining from plasma membrane staining, and the filipin-positive area was quantified on an image-by-image basis using ImageJ software. Each image was acquired with a ×20 objective, and there were ~60 cells per image.

SUPPLEMENTAL INFORMATION

Supplemental Information includes three figures and Supplemental Experimental Procedures and can be found with this article online at http://dx.doi.org/10.1016/j.chembiol.2013.02.009.

ACKNOWLEDGMENTS

We thank Dr. Minoru Ishikawa and Dr. Tappei Takada for critical reading of the manuscript and for helpful comments and Dr. Yukihide Tomari, Dr. Shintaro Iwasaki, and Dr. Mayuko Yoda for allowing us to use some of their facilities and for helpful discussions. This work was supported in part by Grants-in-Aid for JSPS Fellows and for Scientific Research (A) (JSPS KAKENHI grants 2210583 and 22249006).

Received: September 10, 2012
Revised: January 12, 2013
Accepted: February 7, 2013
Published: March 21, 2013

REFERENCES

Aqul, A., Liu, B., Ramirez, C.M., Pieper, A.A., Estill, S.J., Burns, D.K., Liu, B., Repa, J.J., Turley, S.D., and Dietschy, J.M. (2011). Unesterified cholesterol accumulation in late endosomes/lysosomes causes neurodegeneration and is prevented by driving cholesterol export from this compartment. J. Neurosci. *31*, 9404–9413.

Ban, H.S., Shimizu, K., Minegishi, H., and Nakamura, H. (2010). Identification of HSP60 as a primary target of o-carboranylphenoxyacetanilide, an HIF-1alpha inhibitor. J. Am. Chem. Soc. *132*, 11870–11871.

Bolte, S., and Cordelières, F.P. (2006). A guided tour into subcellular colocalization analysis in light microscopy. J. Microsc. *224*, 213–232.

Carstea, E.D., Morris, J.A., Coleman, K.G., Loftus, S.K., Zhang, D., Cummings, C., Gu, J., Rosenfeld, M.A., Pavan, W.J., Krizman, D.B., et al. (1997). Niemann-Pick C1 disease gene: homology to mediators of cholesterol homeostasis. Science *277*, 228–231.

Côté, M., Misasi, J., Ren, T., Bruchez, A., Lee, K., Filone, C.M., Hensley, L., Li, Q., Ory, D., Chandran, K., and Cunningham, J. (2011). Small molecule inhibitors reveal Niemann-Pick C1 is essential for Ebola virus infection. Nature *477*, 344–348.

Davidson, C.D., Ali, N.F., Micsenyi, M.C., Stephney, G., Renault, S., Dobrenis, K., Ory, D.S., Vanier, M.T., and Walkley, S.U. (2009). Chronic cyclodextrin treatment of murine Niemann-Pick C disease ameliorates neuronal cholesterol and glycosphingolipid storage and disease progression. PLoS ONE *4*, e6951.

Davies, J.P., and Ioannou, Y.A. (2000). Topological analysis of Niemann-Pick C1 protein reveals that the membrane orientation of the putative sterol-sensing domain is identical to those of 3-hydroxy-3-methylglutaryl-CoA reductase and sterol regulatory element binding protein cleavage-activating protein. J. Biol. Chem. *275*, 24367–24374.

Davies, J.P., Chen, F.W., and Ioannou, Y.A. (2000). Transmembrane molecular pump activity of Niemann-Pick C1 protein. Science *290*, 2295–2298.

Deffieu, M.S., and Pfeffer, S.R. (2011). Niemann-Pick type C 1 function requires lumenal domain residues that mediate cholesterol-dependent NPC2 binding. Proc. Natl. Acad. Sci. USA *108*, 18932–18936.

Fan, J.Q. (2003). A contradictory treatment for lysosomal storage disorders: inhibitors enhance mutant enzyme activity. Trends Pharmacol. Sci. *24*, 355–360.

Gelsthorpe, M.E., Baumann, N., Millard, E., Gale, S.E., Langmade, S.J., Schaffer, J.E., and Ory, D.S. (2008). Niemann-Pick type C1 I1061T mutant encodes a functional protein that is selected for endoplasmic reticulum-associated degradation due to protein misfolding. J. Biol. Chem. *283*, 8229–8236.

Griffin, L.D., Gong, W., Verot, L., and Mellon, S.H. (2004). Niemann-Pick type C disease involves disrupted neurosteroidogenesis and responds to allopregnanolone. Nat. Med. *10*, 704–711.

Hosoya, T., Hiramatsu, T., Ikemoto, T., Nakanishi, M., Aoyama, H., Hosoya, A., Iwata, T., Maruyama, K., Endo, M., and Suzuki, M. (2004). Novel bifunctional probe for radioisotope-free photoaffinity labeling: compact structure comprised of photospecific ligand ligation and detectable tag anchoring units. Org. Biomol. Chem. *2*, 637–641.

Hua, X., Nohturfft, A., Goldstein, J.L., and Brown, M.S. (1996). Sterol resistance in CHO cells traced to point mutation in SREBP cleavage-activating protein. Cell *87*, 415–426.

Infante, R.E., Abi-Mosleh, L., Radhakrishnan, A., Dale, J.D., Brown, M.S., and Goldstein, J.L. (2008a). Purified NPC1 protein. I. Binding of cholesterol and oxysterols to a 1278-amino acid membrane protein. J. Biol. Chem. *283*, 1052–1063.

Infante, R.E., Radhakrishnan, A., Abi-Mosleh, L., Kinch, L.N., Wang, M.L., Grishin, N.V., Goldstein, J.L., and Brown, M.S. (2008b). Purified NPC1 protein: II. Localization of sterol binding to a 240-amino acid soluble luminal loop. J. Biol. Chem. *283*, 1064–1075.

Infante, R.E., Wang, M.L., Radhakrishnan, A., Kwon, H.J., Brown, M.S., and Goldstein, J.L. (2008c). NPC2 facilitates bidirectional transfer of cholesterol between NPC1 and lipid bilayers, a step in cholesterol egress from lysosomes. Proc. Natl. Acad. Sci. USA *105*, 15287–15292.

Ioannou, Y.A. (2001). Multidrug permeases and subcellular cholesterol transport. Nat. Rev. Mol. Cell Biol. *2*, 657–668.

Ishii, S., Kase, R., Sakuraba, H., and Suzuki, Y. (1993). Characterization of a mutant alpha-galactosidase gene product for the late-onset cardiac form of Fabry disease. Biochem. Biophys. Res. Commun. *197*, 1585–1589.

Ko, D.C., Gordon, M.D., Jin, J.Y., and Scott, M.P. (2001). Dynamic movements of organelles containing Niemann-Pick C1 protein: NPC1 involvement in late endocytic events. Mol. Biol. Cell *12*, 601–614.

Kuwabara, P.E., and Labouesse, M. (2002). The sterol-sensing domain: multiple families, a unique role? Trends Genet. *18*, 193–201.

Kwon, H.J., Abi-Mosleh, L., Wang, M.L., Deisenhofer, J., Goldstein, J.L., Brown, M.S., and Infante, R.E. (2009). Structure of N-terminal domain of NPC1 reveals distinct subdomains for binding and transfer of cholesterol. Cell *137*, 1213–1224.

Liu, R., Lu, P., Chu, J.W., and Sharom, F.J. (2009a). Characterization of fluorescent sterol binding to purified human NPC1. J. Biol. Chem. *284*, 1840–1852.

Liu, B., Turley, S.D., Burns, D.K., Miller, A.M., Repa, J.J., and Dietschy, J.M. (2009b). Reversal of defective lysosomal transport in NPC disease ameliorates liver dysfunction and neurodegeneration in the npc1-/- mouse. Proc. Natl. Acad. Sci. USA *106*, 2377–2382.

Loftus, S.K., Morris, J.A., Carstea, E.D., Gu, J.Z., Cummings, C., Brown, A., Ellison, J., Ohno, K., Rosenfeld, M.A., Tagle, D.A., et al. (1997). Murine model of Niemann-Pick C disease: mutation in a cholesterol homeostasis gene. Science *277*, 232–235.

Loo, T.W., and Clarke, D.M. (1997). Correction of defective protein kinesis of human P-glycoprotein mutants by substrates and modulators. J. Biol. Chem. *272*, 709–712.

Loo, T.W., and Clarke, D.M. (2007). Chemical and pharmacological chaperones as new therapeutic agents. Expert Rev. Mol. Med. *9*, 1–18.

MacEwan, D.J., and Milligan, G. (1996). Inverse agonist-induced up-regulation of the human beta2-adrenoceptor in transfected neuroblastoma X glioma hybrid cells. Mol. Pharmacol. *50*, 1479–1486.

MacKinnon, A.L., Garrison, J.L., Hegde, R.S., and Taunton, J. (2007). Photoleucine incorporation reveals the target of a cyclodepsipeptide inhibitor of cotranslational translocation. J. Am. Chem. Soc. *129*, 14560–14561.

Morello, J.P., Salahpour, A., Laperrière, A., Bernier, V., Arthus, M.F., Lonergan, M., Petäjä-Repo, U., Angers, S., Morin, D., Bichet, D.G., and Bouvier, M. (2000a). Pharmacological chaperones rescue cell-surface expression and function of misfolded V2 vasopressin receptor mutants. J. Clin. Invest. *105*, 887–895.

Morello, J.P., Petäjä-Repo, U.E., Bichet, D.G., and Bouvier, M. (2000b). Pharmacological chaperones: a new twist on receptor folding. Trends Pharmacol. Sci. *21*, 466–469.

Motamed, M., Zhang, Y., Wang, M.L., Seemann, J., Kwon, H.J., Goldstein, J.L., and Brown, M.S. (2011). Identification of luminal Loop 1 of Scap protein as the sterol sensor that maintains cholesterol homeostasis. J. Biol. Chem. *286*, 18002–18012.

Naureckiene, S., Sleat, D.E., Lackland, H., Fensom, A., Vanier, M.T., Wattiaux, R., Jadot, M., and Lobel, P. (2000). Identification of HE1 as the second gene of Niemann-Pick C disease. Science *290*, 2298–2301.

Neufeld, E.B., Wastney, M., Patel, S., Suresh, S., Cooney, A.M., Dwyer, N.K., Roff, C.F., Ohno, K., Morris, J.A., Carstea, E.D., et al. (1999). The Niemann-Pick C1 protein resides in a vesicular compartment linked to retrograde transport of multiple lysosomal cargo. J. Biol. Chem. *274*, 9627–9635.

Ninomiya, H. (2006). Intracellular cholesterol transport by NPC1/NPC2: Mysteries of Niemann-Pick disease type C. In Functional and Structural Biology on the Lipo-Network, K. Morikawa and S. Tate, eds. (Kerala, India: Transworld Research Network), pp. 1–15.

Ohgami, N., Ko, D.C., Thomas, M., Scott, M.P., Chang, C.C., and Chang, T.Y. (2004). Binding between the Niemann-Pick C1 protein and a photoactivatable cholesterol analog requires a functional sterol-sensing domain. Proc. Natl. Acad. Sci. USA *101*, 12473–12478.

Ohsaki, Y., Sugimoto, Y., Suzuki, M., Hosokawa, H., Yoshimori, T., Davies, J.P., Ioannou, Y.A., Vanier, M.T., Ohno, K., and Ninomiya, H. (2006). Cholesterol depletion facilitates ubiquitylation of NPC1 and its association with SKD1/Vps4. J. Cell Sci. *119*, 2643–2653.

Ory, D.S. (2000). Niemann-Pick type C: a disorder of cellular cholesterol trafficking. Biochim. Biophys. Acta *1529*, 331–339.

Patterson, M.C., Vanier, M.T., Suzuki, K., Morris, J.A., Carstea, E., Neufeld, E.B., Blanchette-Mackie, J.E., and Pentchev, P.G. (2001). Niemann-Pick disease type C: A lipid trafficking disorder. In The Metabolic and Molecular Bases of Inherited Disease, Eighth Edition, C.R. Scriver, A.L. Beaudet, W.S. Sly, D. Valle, B. Childs, K.W. Kinzler, and B. Vogelstein, eds. (New York: McGraw–Hill), pp. 3611–3633.

Patterson, M.C., Vecchio, D., Prady, H., Abel, L., and Wraith, J.E. (2007). Miglustat for treatment of Niemann-Pick C disease: a randomised controlled study. Lancet Neurol. *6*, 765–772.

Pentchev, P.G., Comly, M.E., Kruth, H.S., Vanier, M.T., Wenger, D.A., Patel, S., and Brady, R.O. (1985). A defect in cholesterol esterification in Niemann-Pick disease (type C) patients. Proc. Natl. Acad. Sci. USA *82*, 8247–8251.

Pipalia, N.H., Cosner, C.C., Huang, A., Chatterjee, A., Bourbon, P., Farley, N., Helquist, P., Wiest, O., and Maxfield, F.R. (2011). Histone deacetylase inhibitor treatment dramatically reduces cholesterol accumulation in Niemann-Pick type C1 mutant human fibroblasts. Proc. Natl. Acad. Sci. USA *108*, 5620–5625.

Ramsay, D., Bevan, N., Rees, S., and Milligan, G. (2001). Detection of receptor ligands by monitoring selective stabilization of a Renilla luciferase-tagged, constitutively active mutant, G-protein-coupled receptor. Br. J. Pharmacol. *133*, 315–323.

Rosenbaum, A.I., and Maxfield, F.R. (2011). Niemann-Pick type C disease: molecular mechanisms and potential therapeutic approaches. J. Neurochem. *116*, 789–795.

Scott, C., Higgins, M.E., Davies, J.P., and Ioannou, Y.A. (2004). Targeting of NPC1 to late endosomes involves multiple signals, including one residing within the putative sterol-sensing domain. J. Biol. Chem. *279*, 48214–48223.

Sleat, D.E., Wiseman, J.A., El-Banna, M., Price, S.M., Verot, L., Shen, M.M., Tint, G.S., Vanier, M.T., Walkley, S.U., and Lobel, P. (2004). Genetic evidence for nonredundant functional cooperativity between NPC1 and NPC2 in lipid transport. Proc. Natl. Acad. Sci. USA *101*, 5886–5891.

Tseng, T.T., Gratwick, K.S., Kollman, J., Park, D., Nies, D.H., Goffeau, A., and Saier, M.H., Jr. (1999). The RND permease superfamily: an ancient, ubiquitous and diverse family that includes human disease and development proteins. J. Mol. Microbiol. Biotechnol. *1*, 107–125.

Wang, M.L., Motamed, M., Infante, R.E., Abi-Mosleh, L., Kwon, H.J., Brown, M.S., and Goldstein, J.L. (2010). Identification of surface residues on Niemann-Pick C2 essential for hydrophobic handoff of cholesterol to NPC1 in lysosomes. Cell Metab. *12*, 166–173.

Watari, H., Blanchette-Mackie, E.J., Dwyer, N.K., Glick, J.M., Patel, S., Neufeld, E.B., Brady, R.O., Pentchev, P.G., and Strauss, J.F., 3rd. (1999a). Niemann-Pick C1 protein: obligatory roles for N-terminal domains and lysosomal targeting in cholesterol mobilization. Proc. Natl. Acad. Sci. USA *96*, 805–810.

Watari, H., Blanchette-Mackie, E.J., Dwyer, N.K., Watari, M., Neufeld, E.B., Patel, S., Pentchev, P.G., and Strauss, J.F., 3rd. (1999b). Mutations in the leucine zipper motif and sterol-sensing domain inactivate the Niemann-Pick C1 glycoprotein. J. Biol. Chem. *274*, 21861–21866.

Watari, H., Blanchette-Mackie, E.J., Dwyer, N.K., Watari, M., Burd, C.G., Patel, S., Pentchev, P.G., and Strauss, J.F., 3rd. (2000). Determinants of NPC1 expression and action: key promoter regions, posttranscriptional control, and the importance of a "cysteine-rich" loop. Exp. Cell Res. *259*, 247–256.

Xie, X., Brown, M.S., Shelton, J.M., Richardson, J.A., Goldstein, J.L., and Liang, G. (2011). Amino acid substitution in NPC1 that abolishes cholesterol binding reproduces phenotype of complete NPC1 deficiency in mice. Proc. Natl. Acad. Sci. USA *108*, 15330–15335.

Yamamoto, T., Ninomiya, H., Matsumoto, M., Ohta, Y., Nanba, E., Tsutsumi, Y., Yamakawa, K., Millat, G., Vanier, M.T., Pentchev, P.G., and Ohno, K. (2000). Genotype-phenotype relationship of Niemann-Pick disease type C: a possible correlation between clinical onset and levels of NPC1 protein in isolated skin fibroblasts. J. Med. Genet. *37*, 707–712.

Yamamoto, T., Feng, J.H., Higaki, K., Taniguchi, M., Nanba, E., Ninomiya, H., and Ohno, K. (2004). Increased NPC1 mRNA in skin fibroblasts from Niemann-Pick disease type C patients. Brain Dev. *26*, 245–250.

Zhang, M., Dwyer, N.K., Love, D.C., Cooney, A., Comly, M., Neufeld, E., Pentchev, P.G., Blanchette-Mackie, E.J., and Hanover, J.A. (2001a). Cessation of rapid late endosomal tubulovesicular trafficking in Niemann-Pick type C1 disease. Proc. Natl. Acad. Sci. USA *98*, 4466–4471.

Zhang, M., Dwyer, N.K., Neufeld, E.B., Love, D.C., Cooney, A., Comly, M., Patel, S., Watari, H., Strauss, J.F., 3rd, Pentchev, P.G., et al. (2001b). Sterol-modulated glycolipid sorting occurs in Niemann-pick C1 late endosomes. J. Biol. Chem. *276*, 3417–3425.

